Hydrological pre-feasibility assessment for the Romuku hydropower plant Central Sulawesi, Indonesia

May 2015

Author
J.E. Hunink
S. Contreras
P. Droogers

Client
Hydropower Evolutions

Report FutureWater: 141

FutureWater
Costerweg 1G
6702 AA Wageningen
The Netherlands

+31 (0)317 460050

info@futurewater.nl

www.futurewater.nl

Preface

Following the successful development of other hydropower facilities in Indonesia, a new project aims to study the potential of the “Romuku” run-of-river power plant in Central Sulawesi. The project should turn this renewable energy opportunity into a source of economic empowerment for the region and a carbon-emission-free and reliable source of electricity for the people of Sulawesi.

A first step is to undertake a pre-Feasibility Study which will result in a go no-go decision for a more detailed Feasibility Study. This study encompasses various components. FutureWater carries out the hydrological assessment of this pre-feasibility phase, supporting Hydropower Evolutions in the overall assessment. The objective is to undertake a first order analysis on the expected flow at the inlet of the proposed Romuku run-of-river power plant.

Summary

This report describes the methods and results of the hydrological assessment that was carried out for the pre-Feasibility Study of the Romuku hydropower plant, Sulawesi, Indonesia. Due to the lack of reliable streamflow data, the assessment was based on hydrological modelling of the basin upstream of the point of interest. Principally global datasets were used for the biophysical input requirements of the hydrological modelling.

The principal output is a flow-duration curve based on multiple model simulations. The flow duration curve includes confidence bounds based on the uncertainties that exist currently in rainfall data, evapotranspiration and runoff mechanisms. These uncertainties were also assessed for the monthly flow regime, based on the daily model simulations.

From this hydrological assessment, a number of recommendations are put forward that aim at increasing the level of accuracy in the outcomes and narrow the uncertainty range for the following feasibility stage. Recommendations are done for data improvements, model improvements and field validation.

Table of contents

Tables

Figures

1 Introduction

There is great potential for hydropower in Indonesia, and this natural resource is likely to be increasingly utilised for power generation in the future. With the escalating demand for energy, government authorities are keen to harness renewable energy from the country's many rivers. Often these projects aim at remote communities for which connecting to the national power grid is prohibitively expensive. Thus, local hydropower production is an attractive and sometimes viable option. Critical is to conduct accurate feasibility assessments for hydropower generation at the different potential sites of interest.

This project aims to study the potential of the "Romuku" run-of-river power plant in Central Sulawesi, Indonesia (Figure 1). The project should turn this renewable energy opportunity into a source of economic empowerment for the region and a carbon-emission-free and reliable source of electricity for the people of Sulawesi.

Figure 1. Location of proposed site of Romuku hydropower plant

A first step for this project is to undertake a pre-Feasibility Study which will result in a go no-go decision for a more detailed Feasibility Study. This study encompasses various components. This report summarizes the hydrological assessment carried out by FutureWater. The objective is to undertake a first order assessment on the expected flow at the inlet of the proposed Romuku run-of-river power plant.

2 Methodology

2.1 Summary of approach

Available data for the proposed site are limited. At this stage, no useful streamflow data are available to derive flow statistics and a flow duration curve. As alternative a hydrological rainfall-runoff model can be used to generate discharge data from which flow duration curves can be derived. Combining available local datasets and global datasets on the biophysical characteristics of the basin, such a model can deliver daily streamflow simulations.

It is proposed to use the HEC-HMS in this pre-feasibility phase. HEC-HMS is a hydrological model that simulates the rainfall-runoff at any point within a watershed given physical characteristics of the watershed. It can be used for studying interventions and for watershed management to determine the effect on the magnitude, quantity, and timing of runoff at different points of interest. It is one of the most commonly used rainfall-runoff models, freely available and flexible in data requirements.

This pre-Feasibility Study will result in a first order assessment of the expected flows into the proposed site location. For the Feasibility Study a more extensive analysis is needed, including more field data, detailed analysis of spatial rainfall patterns, more advanced rainfall-runoff model, advanced calibration of model, and an analysis of potential threats to future water flows (land-use changes, climate change).

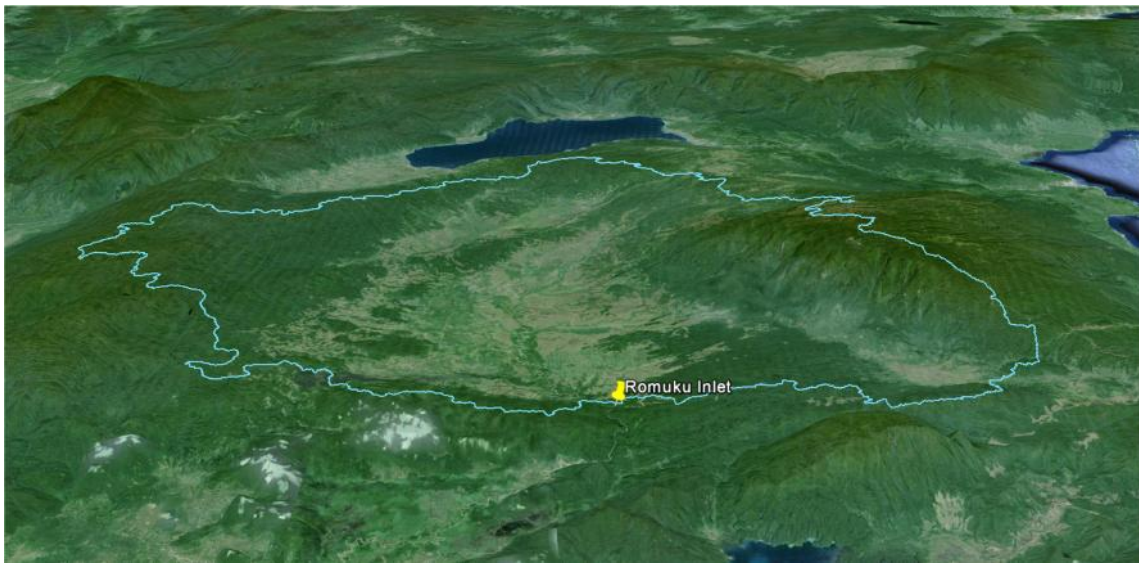

Figure 2. Google Earth view of basin of study site

2.2 Model selection

The flow-duration curve (FDC) is the most common tool used for preliminary studies of run-of hydropower plant capacity. The area below the FDC with as upper limit the turbine-capacity, is used to asses primary (firm power) and secondary power (Figure 3).

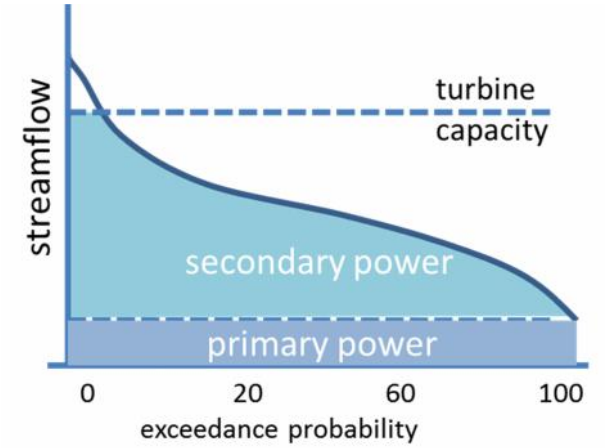

Figure 3. Example use of flow duration curve for feasibility assessment of run-of-river hydropower facilities

If sufficient streamflow data are available, FDCs can be constructed directly from observations. If not, FDCs need to be derived from hydrological analysis and/or modelling. A wide range of methods and models can be employed. The selection of these models depend on the level of accuracy and final purpose of the FDC. They can be constructed from monthly data, but daily FDCs may be preferable if considerable streamflow variability exists on a daily scale.

For daily streamflow variability assessments and construction of FDCs, a hydrological model needs to be employed. The model requirements for the pre-feasibility analysis of the Romuku hydropower plant are:

- Allowing long-term continuous simulations
- Allowing discretization in different sub-basins
- Model with proven track record for similar assessments
- Flexibility for uncertainty assessments

Based on these requirements, the HEC-HMS model was selected. The HEC-HMS model draws on several decades of experience with hydrologic simulation software, and is developed and supported by the U.S. Army Corps of Engineers (USACE). HEC-HMS is a hydrological model that simulates the rainfall-runoff at any point within a watershed given physical characteristics of the watershed. It can be used for studying interventions and for watershed management to determine the effect on the magnitude, quantity, and timing of runoff at points of interest. Results from an HMS model can be used by a number of other programs to determine impact in areas such as water quality and flood damage.

HEC-HMS has been applied in a wide range of geographic areas for solving the widest possible range of problems. This includes large river basin water supply and flood hydrology, and small urban or natural watershed runoff. Hydrographs produced by the program are used directly or in conjunction with other software for studies of water availability, urban drainage, flow forecasting, future urbanization impact, reservoir spillway design, flood damage reduction, floodplain regulation, wetlands hydrology, and systems operation.

HMS features a completely integrated work environment including a database integrated in a Geographical Information System (ArcGIS), data entry utilities, computation engine, and results reporting tools. A graphical user interface allows the user seamless movement between the different parts of the program. Time-series, paired, and gridded data are stored in the Data Storage System called HEC-DSS and promoted by USACE.

2.3 Model components

The main components of an HMS model are the Basin Model, Metrological Model, and Control Specifications. The physical representation of watersheds or basins and rivers is configured in the basin model and can be derived from GIS data. Hydrologic elements are connected in a dendritic network to simulate runoff processes. Available elements are: subbasin, reach, junction, reservoir, diversion, source, and sink. Meteorologic data analysis is performed by the meteorologic model and includes precipitation and evapotranspiration. The time span of a simulation is controlled by control specifications, which include a starting date and time, ending date and time, and computation time step.

Hydrologic elements are the building blocks of a basin model. Figure 4 shows the schematic setup for the basin model of this pre-feasibility study. There are eight subbasin elements, three reach elements, and three junction elements in the basin model (see also the map in Figure 15). Each element represents part of the total response of the watershed to precipitation.

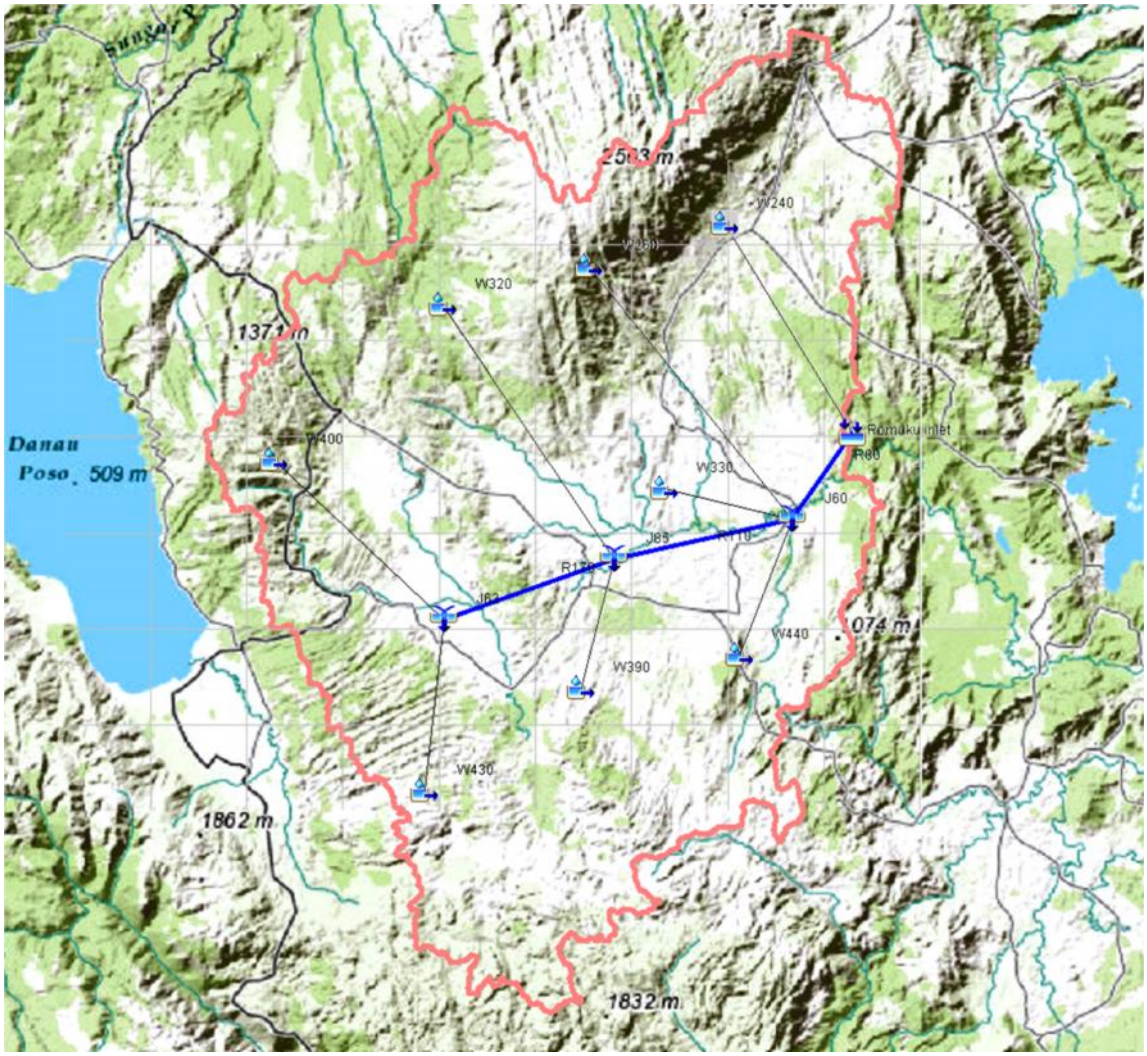

Figure 4. Schematic setup of HEC-HMS model

There are a wide range of methods that can be selected and used in HEC-HMS to describe the hydrological processes. Some of them are only adequate for storm runoff analysis. Others are more focussed on long-term continuous hydrological simulations, as necessary for this study. Table 9 summarizes shortly the selected methods for this study. The following sections provide more details on the model parameterization and model inputs.

Table 1. Selected methods of HEC-HMS for this study

Element	Description
Canopy	The canopy component describes the presence of plants in the landscape, simulating interception and canopy evapotranspiration. For this study, the Simple plant water uptake method was chosen, crop coefficient =1 (tropical systems tend to be energy-limited, not water-limited), and maximum canopy storage assumed 2 mm.
Surface	The Surface component describes the ground surface where water may accumulate. For this study, the Simple Surface method was chosen, with 5 mm of max surface storage.
Loss	This component determines principally the rainfall-runoff partitioning (infiltration, surface runoff and sub-surface runoff). For this study, the deficit and constant method was used, that allows dynamic simulations and conserves mass. The constant rate (similar to maximum infiltration rate) was extracted from soil maps. The maximum storage was set at 300mm.
Baseflow	Several baseflow methods are available in HEC-HMS. For this study, the linear reservoir method was chosen as for continuous simulation it is necessary that the method conserves mass. Coefficients were based on values that can be reasonably expected for this type of tropical systems.
Routing	Routing method propagates water through the channels. For this study, the Muskingum method was used. Parameter Muskingum K was based on channel length, estimated hydraulic radius and slope, and for Muskingum X, a typical value was chosen for floodplain rivers (0.2).

2.4 Model inputs

Principal model input datasets required for HEC-HMS are:

- Rainfall
- Evapotranspiration
- Land use
- Soil

The following sections describe the data quality assessment and data pre-processing that was carried out.

2.4.1 Rainfall

2.4.1.1 Meteorological stations

The set of meteorological station with daily rainfall data used in this study is comprised by four local meteorological stations (#Mayoa, #Kolo, #Tolae and #Lembo), and the station STN970960 (#Poso) from the GSOD-NCDC worldwide database. Location and basic statistics are shown in Table 2, Table 3 and Table 4. Rainfall data from local station were provided by local authorities,

while data from the GSOD station was collected from the GSOD-NCDC database through the NOAA webpage (http://www.climate.gov/).

Table 2. Meteorological stations available in the study area.

Meteo Station	Source	Latitude	Longitude	Altitude (m.a.s.l.)	Period with data	Missing values (1985-2013)
Mayoa (#Mayoa)	Local	-2.1449	12.03320	562	1985 – 1999 2002 - 2011	1492
Kolondale (#Kolo)	Local	-2.0197	121.3448	5	1985-2002 2009-2013	2206
Tolae (#Tolae)	Local	-0.9864	120.3320	8	1985 - 2013	258
Poso-Kasinguncu (#Poso)	GSOD-NCDC	-1.4210	120.6500	16	1993 – 2000 2008 – 2013	6214
Lembontanara (#Lembo)	Local	-1.9498	120.9390	324	2007 – 2013	8035

Table 3. Number daily gaps reported for the 1985-2013 period. White-black scale showing increasing number of missing values.

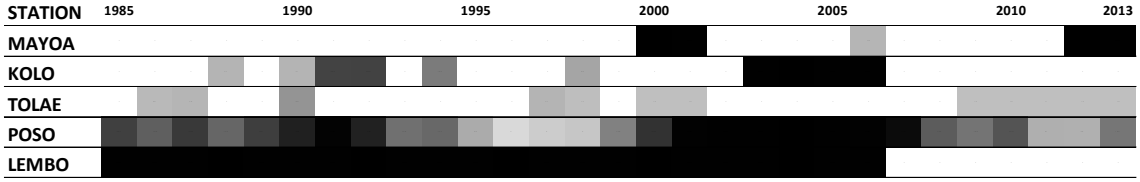

As can be seen in Table 3, the Lembontanara station covers a very short period. Also, comparing the few years with data of the Mayoa station, it appeared that the similarity is so high that it may have been majorly reconstructed from the Mayoa station, and not from actually observed data at this location. For these two reasons, this station was discarded. Also the Poso station was finally rejected for this study due to the high number of missing values observed for the 1985-2013 period.

Because of its proximity to the basin, #Mayoa and #Kolo stations were submited to a: (1) reconstruction and quality-control, and (2) and a preliminary homogeneity test to detect changepoints in the monthly-annual reconstructed timeseries. The Tolae station was considered as second-order neighbour station which was used for filling small gaps not filled with #Mayoa and #Kolo information.

Table 4. Basic yearly statistics for the meteorological stations selected.

Meteo Station	Mean Annual Rainfall (mm)	Coefficient of variation	Percentile 10	Percentile 90	Days with rainfall >1mm	Mean annual rainfall TRMM
#Mayoa*	3764	20.9	2771	4701	204	4048
#Kolo*	2683	46.6	973	4503	201	2427
#Tolae**	1286	46.5	591	2104	85	2640

* Values computed from the filled timeserie (see section 2.4.1.2)

** Values computed from the original timeserie. Years with more than 12 gaps were not included for the statistics.

2.4.1.2 Reconstruction and gap filling

Both, #Kolo and #Mayoa were considered here as first-order stations from which to generate daily patterns of rainfall at the subbasin scale. Daily gaps in both stations were filled using a one-by-one average monthly-ratio approach. The computation of the monthly ratios from the interannual-average timeseries gives a very valuable reduction of the noise during the filling procedure. When a gap is found in the daily timeserie of the target station, the missing value is filled as:

$$P_{d,target} = P_{d,reference} * \frac{P_{m,target}}{P_{m,reference}}$$

were, $P_{d,target}$ is the gap day to be filled in the target station, $P_{d,reference}$ is the daily rainfall in the reference station and, $P_{m,target}/P_{m,reference}$ is the monthly ratio computed from the mean monthly timeseries observed at both stations.

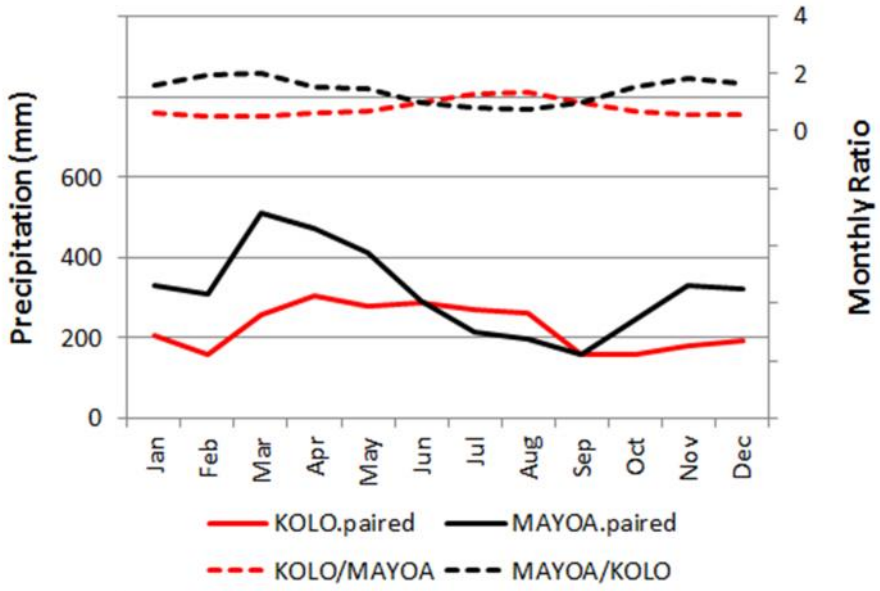

Figure 5. Average monthly precipitation (1985-2013) timeseries recorded at #Mayoa and #Kolo stations (continuous lines), and monthly ratios (dashed line) adopted for filling daily gaps.

In September-2006 no data was recorded at both #Mayoa and #Kolo stations. For filling this period, a linear regression between the target station (#Mayoa or #Kolo) and the #Tolae station was computed from the daily timeseries.

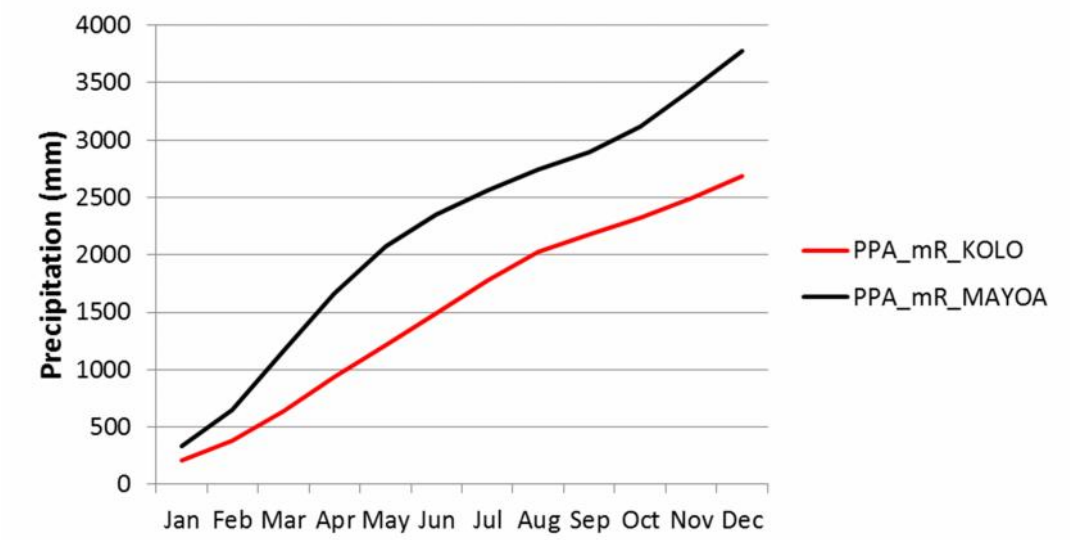

Figure 6. Average monthly accumulated precipitation for #Mayoa and #Kolo stations.

2.4.1.3 Tests of homogenization

A homogeneous climate series is defined as one where variations are caused only by changes in weather and climate [*González-Rouco et al.*, 2001]. In general, accurate long-term climate analysis requires homogeneous data, and then potential inhomogeneities resulting from changes in instruments, locations, observers or other environmental factors must be detected to be excluded or adjusted.

Several statistical tests have been developed that allow detection of inhomogeneities in time series. Some tests are univariant and are directly applied over the candidate or target station (absolute tests), while others use information from reference time series (reference or neighbour stations) that are compared with the candidate series to decide upon its quality (relative tests). A comprehensive review on this topic has been presented by Peterson et al. [1998]. Absolute tests have to be used with care, as the detection of changepoints from individual stations may be caused or masked by real changes in climate [*Peterson et al.*, 1998]. We adopted an absolute and relative parametric test to on the filled #Mayoa and #Kolo monthly and annual timeseries.

The SNHT test is a widely used paremetric test with a strong capacity to detect single shifts of the mean level along a timeserie [*Alexandersson*, 1986; *Peterson et al.*, 1998]. It has been used in wide variety of homogeneity studies (see references provided by [*Khaliq and Ouarda*, 2007]). When it is applied in an absolute way, i.e. considering a station alone, the SNHT test firstly normalize the raw timeserie as

$$Z_i = \frac{X_i - \overline{X}}{\sigma_X}$$

The SNHT test treats the elements in Z as normally distributed. If a changepoint exists, then the original timeserie may be split into two ones which are also assumed to fit a normal distribution. The detection of the change point in the original timeserie is evaluated through the likelihood ration statistic (T) which is computed as [*Alexandersson*, 1986]

$$T_0 = \max_{1 \le c < n} \{\widetilde{T}_c\}, \qquad \widetilde{T}_c = c * \overline{[illegible]}_1 + (n-c) * \overline{[illegible]}_2$$

Where c is the timestep in which occurs the breakpoint, n is the total of timesteps in the serie, and $\overline{Z1}$ y $\overline{Z2}$ denotes sample means before and after time c.

A potential breakpoint is considered significant when T0 is higher than the 90-95% critical value tabulated for the lenght of the serie. In Figure 7 is illustrated the procedure behind the SNHT test.

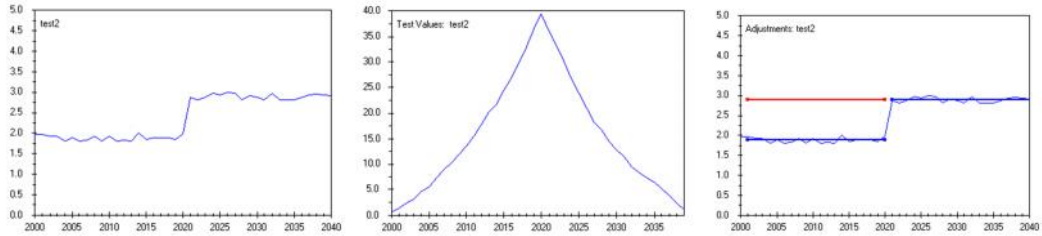

Figure 7. A) Nomalized random serie (n=40) with a single shift of the mean level at the middle of the period. B) T_0 values from the SNHT and critical value for a 95% p-level (dashed red line) , C) Suggested adjusted ratio for erase the shift.

Results from the absolute SHNT test run over the annual timeseries of #Mayoa station are shown in Figure 8.

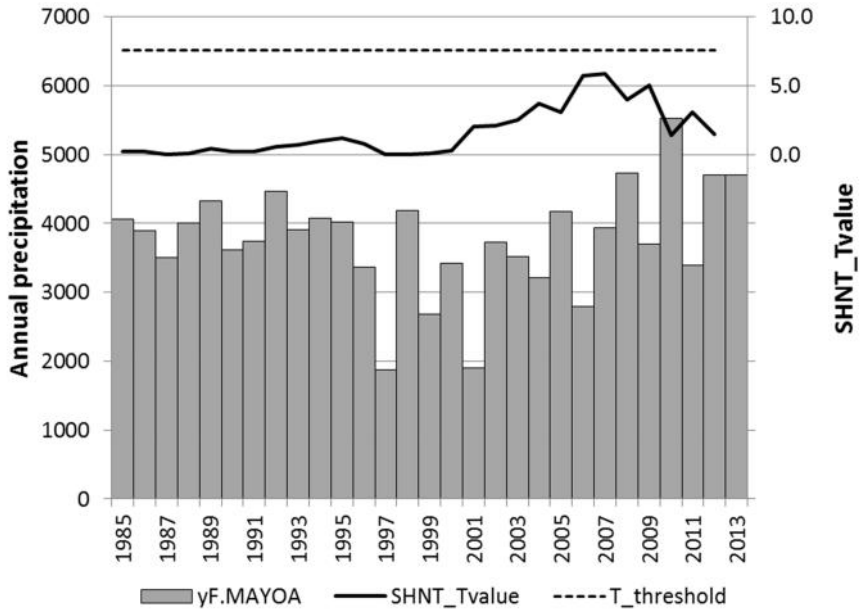

Figure 8. Annual rainfall computed for #Mayoa reconstructed timeseries.

From visual inspection of the annual rainfall data of the Kolo station, it appeared that 1985, 1986, 1989 and 1990 were anonymously low. In order to test this, we did a relative SHNT test taking #Mayoa as the reference station and #Kolo as the candidate station. In relative tests, the variable timeserie that is tested is the ratio between the values of both stations computed as:

$$Q_i = \frac{Y_i}{X_i \overline{Y}/\overline{X}}$$

Where Yi and Xi are the rainfall at the candidate and reference stations respectively, and $\overline{Y}$ and $\overline{X}$ are the average values for the timeserie considered. The Q_i timeserie is standarized and proceeded as was explained before for the absolute test. The analysis confirmed that there were several issues with this dataset. Finally, it was decided to discard this station for this reason, also because its location (near the coast) is most likely less representative for the study area, than the Mayoa station (interior, and closer).

2.4.1.4 Satellite-based rainfall TRMM

Within the basin, high rainfall gradients exist. These spatial patterns should be taken into account and are critical when simulating streamflow from climate datasets. Local isohyet maps were available for Sulawesi (Figure 9). These maps suggest that rainfall amounts are higher in the south-western part of the basin (around 3500 mm) and lower in the northern part (2500 mm).

Figure 9. Extract of study area from local isohyet map for Sulawesi

Nowadays, different satellite-based rainfall products are available that measure rainfall on different timescales. The Tropical Rainfall Measuring Mission (TRMM) is a satellite launched and operated by the US Space Agency (NASA) and the Japanese Aerospace Exploration Agency (JAXA). The satellite mission is focused on providing data on tropical and subtropical

precipitation and to estimate its associated latent heating. TRMM is operational since November 1997 and is releasing products since 1998.

There are different TRMM products with different spatial and temporal resolutions. The 3-hourly and daily products deliver outputs on 25 km spatial resolution. Based on these daily inputs, also monthly products are prepared and available for download.

To obtain a sufficiently spatially detailed distribution of rainfall in this basin, the UCSB's TRMM-based spatial dataset with historical averages of monthly precipitation was extracted from http://www.geog.ucsb.edu/~bodo/TRMM/ . Figure 10 shows the mean annual rainfall for the basin, based on these monthly spatial distributions. Similar to the local isohyet maps, TRMM indicates higher rainfall amounts in the south of the basin, and generally lower amounts in the north. Due to the relatively high spatial resolution, TRMM also detects higher rainfall on the small mountain range in the north of the basin, up to 3000 mm per year.

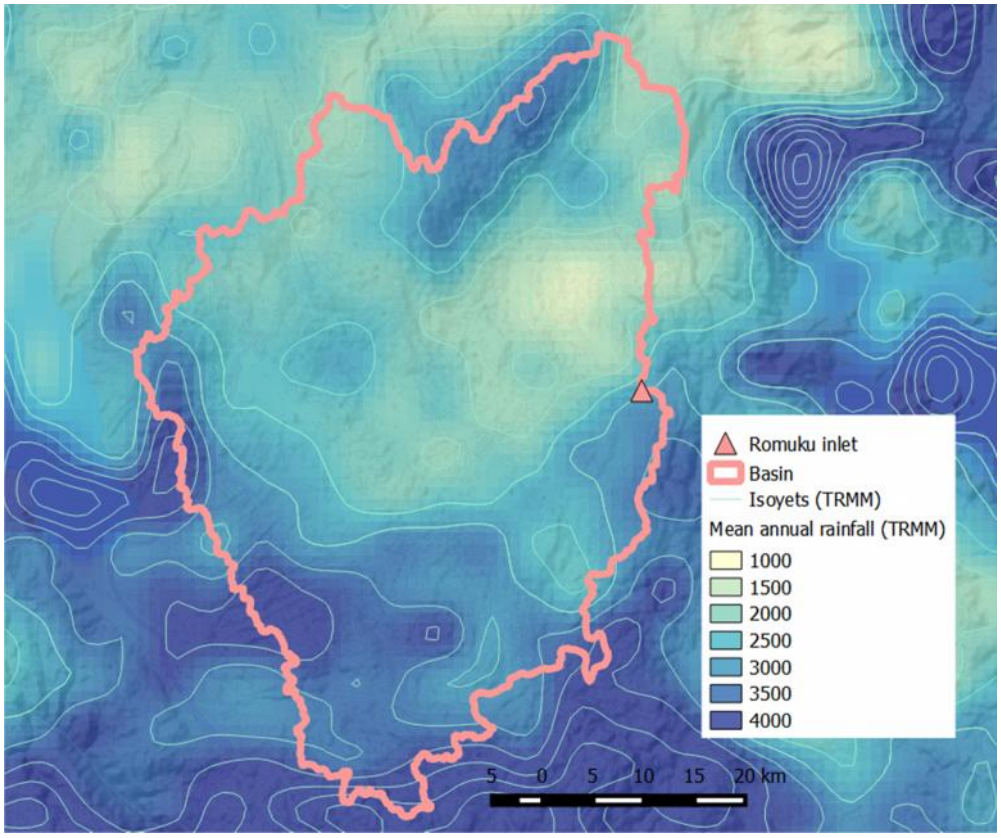

Figure 10. TRMM annual rainfall for study basin

From this TRMM dataset, monthly ratios were computed at the pixel level between each location inside the basin and the TRMM value observed at #Mayoa station. Average values of the ratios computed at each subbasin were finally extracted and used for computing daily rainfall timeseries from the #Mayoa station. Hence, timeseries of daily precipitation at the subbasin scale were computed as:

$$P_{d,HydroID} = P_{d,\#Mayoa} * \frac{\overline{\sum_{t=1}^{n} P_{m,t}}}{P_{m,\#Mayoa}}$$

Where, $P_{d,HydroID}$ is the representative daily precipitation for the subbasin *HydroID*; $P_{d,\#Mayoa}$ is the daily precipitation recorded at the #Mayoa station according the reconstructed daily timeserie; $P_{m,i}$ is the monthly TRMM precipitation observed at pixel i inside the subbasin HydroID, being n the total of pixels included in the basin, and $P_{m,\#Mayoa}$ is the monthly TRMM values observed at the #Mayoa location.

2.4.2 Evapotranspiration

Daily raw data of pan evaporation measurements from 1985 to 2013 at #Mayoa station were extracted from the local available dataset. A preliminary quality assessment consisting of the detection of outliers and the filling of gaps was performed.

Outliers were detected using a threshold value approach. The threshold value was computed as:

$$T_{Epan} = \overline{Epan} + 1.96 * \sigma_{Epan}$$

where, the $\overline{Epan}$ is the daily average of Epan observed along the whole serie, and σ_{Epan} is the standard deviation. Adopting this criteria, T_{Epan} was set in 15 mm/day.

Gaps or outliers were filled at the daily scale using the daily average observed during the corresponding month or, when no data at this month was available, the interannual mean monthly value observed along the whole serie.

Finally, after the quality assessment and the filling procedure the SNHT test was run over the reconstructed annual timeserie. The homogeneity test detected a significant breakpoint at 2001 (Figure 11) which may suggest its adjustment at the time before this breakpoint. We decided to apply the ratio between the average E0 values after and before the breakpoint (0.916) to adjust the original timeseries. Figure 12 shows the original and reconstructed pan evaporation series from the #Mayoa station used in this study.

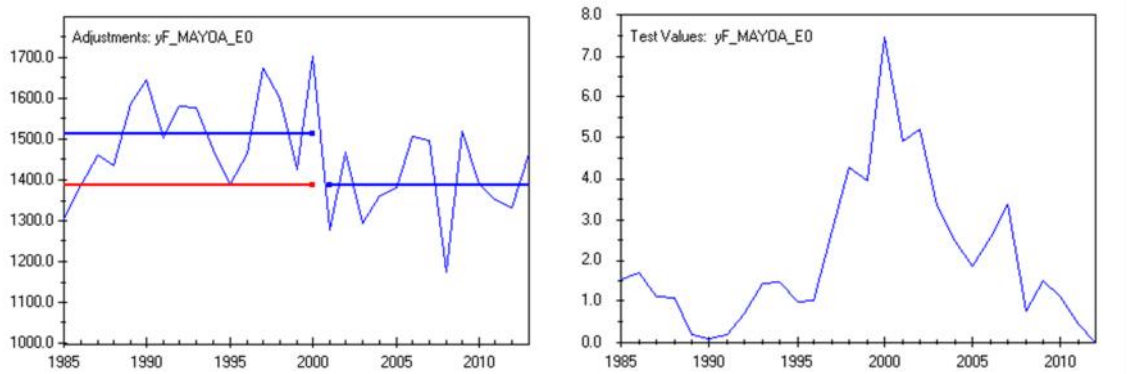

Figure 11. Left: Annual pan evaporation timeserie observed at the #Mayoa station before the homogeneization adjustment. Right: T-value from the SHNT test.

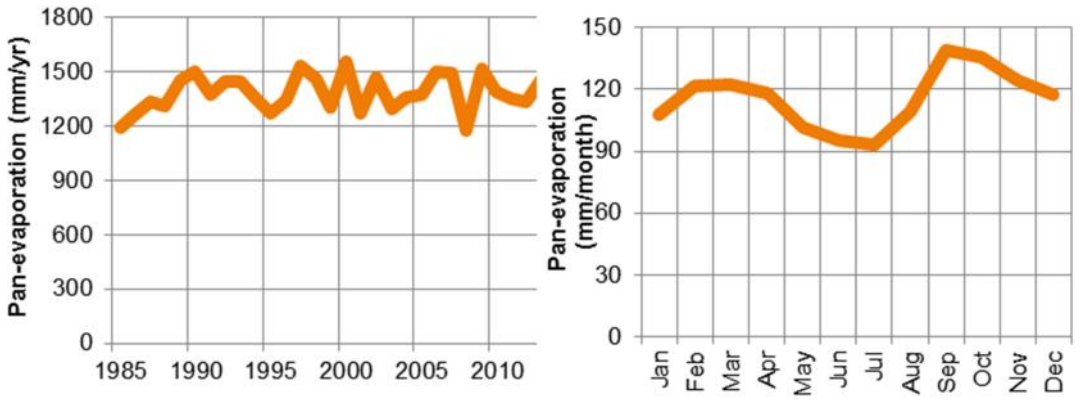

Figure 12. Annual and monthly variability of pan-evaporation

From the documents of the preceding potential study of the Romuku hydropower plant, we interpreted from the calculation tables that an annual ETa of around 2000 mm was estimated. This is considerably higher than the values obtained from the pan-evaporation data (being a good indication of potential evapotranspiration in tropical systems) that show an annual average of around 1400 mm.

2.4.3 Land cover

At this stage, no local dataset on land use was available. Therefore, a global land use dataset was used as input into the hydrological modelling. GlobCover is an ESA initiative in partnership with JRC, EEA, FAO, UNEP, GOFC-GOLD and IGBP. The GlobCover project has developed a service capable of delivering global composite and land cover maps using, as input, observations from the 300 m MERIS sensor on board the ENVISAT satellite mission. The GlobCover service was demonstrated over a period of 19 months (December 2004 - June 2006), for which a set of MERIS Full Resolution (FR) composites (bi-monthly and annual) and a Global Land Cover map are being produced.

The land cover map (version 2.3., 2009) provided by the GlobCover project has been extracted for the study region (Figure 13). Table 5 shows the total area of each of the classes defined in the Globcover dataset, and their relative share.

Table 5. Land use classes, area and percentage of total area in the Romuku catchment (GlobCover)

Land Use Class	Area (km2)	% of total
Rainfed croplands	436	17
Mosaic cropland (50-70%) / vegetation (grassland/shrubland/forest) (20-50%)	801	32
Mosaic vegetation (grassland/shrubland/forest) (50-70%) / cropland (20-50%)	92	4
Closed to open (>15%) broadleaved evergreen or semi-deciduous forest (>5m)	1158	46
Closed to open (>15%) (broadleaved or needleleaved, evergreen or deciduous) shrubland (<5m)	36	1
Total	**2523**	**100**

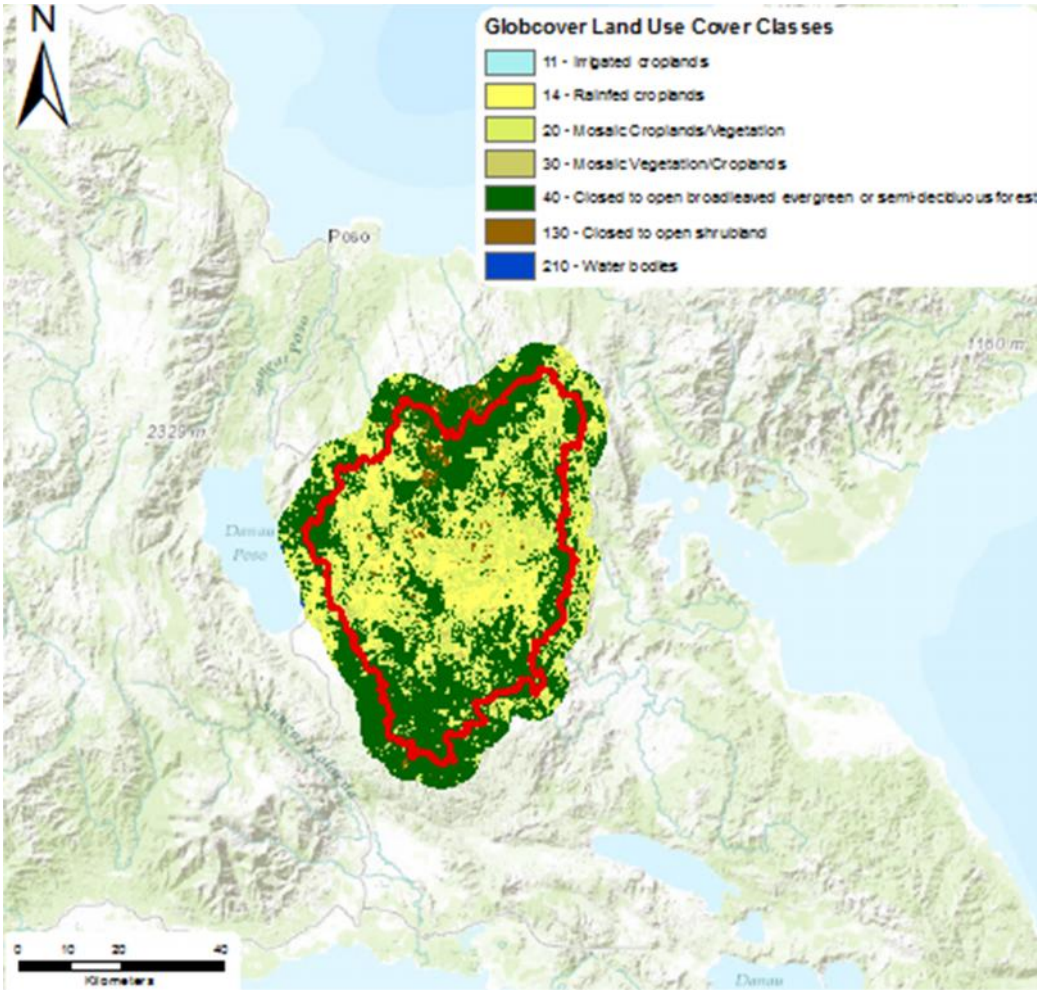

Figure 13. Land cover map of the study area

2.4.4 Soil

FutureWater has co-developed with the International Soil Institute ISRIC the global soil dataset called SoilGrids1km dataset [*Hengl et al.*, 2014]. This dataset offers a range of soil parameters on 1km spatial resoltuion that can be used as input into hydrological modelling. Because local data on soils is lacking at this stage, this dataset was used as input into the hydrological modelling.

For the Loss and Transform method in the HEC-HMS model, the soil classification of the Natural Resource Conservation Service is required. This classification has four Hydrologic Soil Groups based on the soil's runoff potential.

These soil hydrologic groups were derived from soil data of the SoilGrids1km dataset and from the map of soil taxonomic groups of the World Reference Base of 2006. Five taxonomic groups dominate the area (Figure 14, Table 7). General notes on the main characteristics of these soils were extracted from FAO [2001] and the WRB2006 Manual [*FAO*, 2006]. Finally, two additional parameters, the maximum storage capacity and the infiltration rate, were collected into Table 8 at for the main soil taxa found in the basin.

Table 6. Main characteristics of the Hydrological Soil Groups adopted for the Soil Conservation Service Curve Number method.

Hydrological Soil Group	Description	Soil texture	Infiltration rate [mm/h]
HSG A	Low runoff potential: Soils with high infiltration rates. Deep, well-drained sands and gravels.	Deep sand, deep loess, aggregated silts	> 7.62
HSG B	Soils with moderate infiltration rates. Soils moderately deep to deep, moderately well drained to well drained with moderately fine to moderately course textures.	Shallow loess, sandy loam	3.81 – 7.62
HSG C	Soils with slow infiltration rates, a layer that impedes downward movement of water or with moderately fine to fine textures.	Clay loams, shallow sandy loam, soils low in organic content, and soils usually high in clay	1.27 – 3.81
HSG D	High runoff potential: Soils with very slow infiltration rates, a high swelling potential, a permanent high water table, with a claypan or clay layer at or near the surface, and shallow soils over nearly impervious materials. These soils have a very slow rate of water transmission	Soils that swell significantly when wet, heavy plastic clays, and certain saline soils	< 1.27

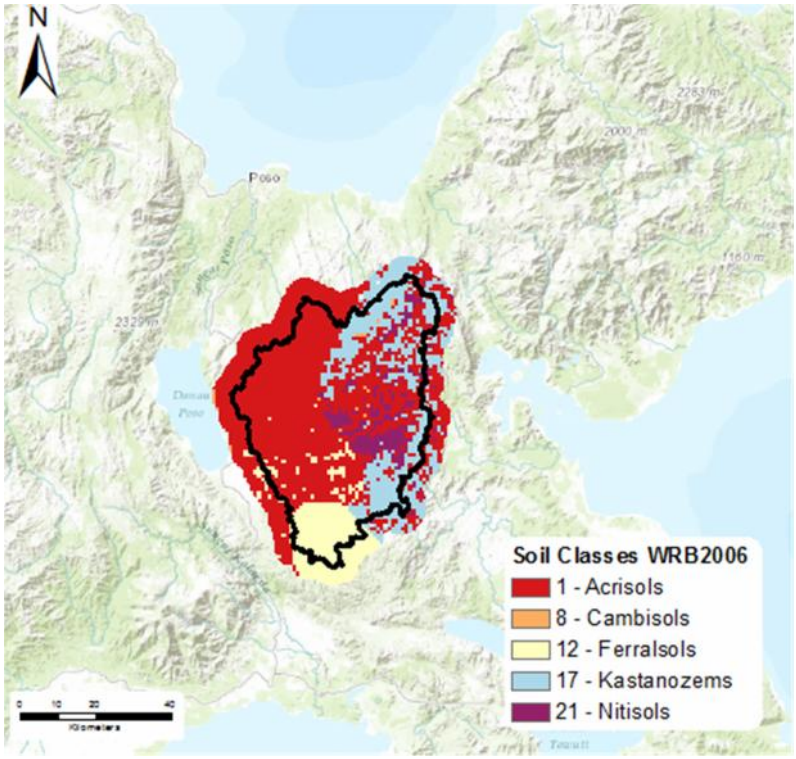

Figure 14. Soil taxonomic groups (WRB2006 code) found in the study basin. Data extracted from the SoilGrids-1km database [*Hengl et al.*, 2014]**.**

Table 7. Soil taxonomic groups reported in the area according the SoilGrid1km database.

Soil taxonomic group	Description	Area (% basin)	SCS soil hydrologic group
Acrisols	Soils with a higher clay content in the subsoil than in the topsoil leading to an argic subsoil horizon. *Environment*: Old land surfaces with hilly or undulating topography, in regions with a wet tropical/monsoonal, subtropical or warm temperate climate. Light forest is the natural vegetation type. *Physical and hydrological characteristics*: Under a protective forest cover have porous surface soils. If the forest is cleared, the valuable A-horizon degrades and slakes to form a hard surface crust which promotes surface erosion. Many Acrisols in low landscape positions show signs of periodic water saturation.	58.7	D
Kastanozems	Kastanozems accommodate dry grassland soils, among them the zonal soils of the short-grass steppe belt, south of the Eurasian tall-grass steppe belt with Chernozems. Similar profile to that of Chernozems but the humus-rich surface horizon is thinner and not as dark as that of the Chernozems and they show more prominent accumulation of secondary carbonates. *Environment*: Dry and warm; flat to undulating grasslands with ephemeral short grasses. *Physical and hydrological characteristics*: They have an intermittent water regime. Low non-capillary porosity promotes high surface runoff rates during and after heavy rainfall events (a 'dead dry horizon' occurs below the limit of wetting). Low permeability to water.	21.9	C
Ferralsols	Ferralsols represent the classical, deeply weathered, red or yellow soils of the humid tropics. These soils have diffuse horizon boundaries, a clay assemblage dominated by low-activity clays (mainly kaolinite) and a high content of sesquioxides. *Environment*: Typically in level to undulating land of Pleistocene age or older; less common on younger, easily weathering rocks. Perhumid or humid tropics. *Physical and hydrological characteristics*: clayey (a consequence of advanced weathering) and have strong water retention at permanent wilting point while the presence of micro-aggregates reduces moisture storage at field capacity. Stable micro-aggregates explain the excellent porosity, good permeability and favourable infiltration rates.	12.3	A
Nitisols	Nitisols are deep, well-drained, red, tropical soils with diffuse horizon boundaries and a subsurface horizon with more than 30 percent clay and moderate to strong angular blocky structure elements that easily fall apart into characteristic shiny, polyhedric (nutty) elements. *Environment*: Predominantly found in level to hilly land under tropical rain forest or savannah vegetation *Physical and hydrological characteristics*: Free-draining soils and permeable to water (50-60 percent pores).	6.5	A
Cambisols	Cambisols combine soils with at least an incipient subsurface soil formation. *Environment*: Medium altitudes in hilly and mountain regions but also in deposition areas and in eroding lands at lower altitude where they occur alongside genetically mature residual soils. *Physical and hydrological characteristics*: Soil texture is loamy to clayey. Good structural stability, a high porosity, a good water holding capacity and good internal drainage. Many exceptions.	0.4	C

Table 8. Main hydrological parameters for the soil taxa dominating the study area.

Soil taxonomic group	Maximum storage (mm)	Infiltration rate (mm/h)
Acrisols	500[1)]	0.5
Kastanozems	225[2)]	2.5
Ferralsols	250[3)]	10.0
Nitisols	300[4)]	10.0
Cambisols	75[5)]	2.5

1) For soil depths of 1 m. [*Wenzel et al.*, 1998]
2) Soil depth: 0.75 m; SWS/depth ratio = 0.30
3) Soil depth: 2.5 m; WHC/depth ratio = 0.10
4) Soil depth: 2.0 m; WHC/depth ratio = 0.15
5) Soil depth: 0.5 m; WHC/depth ratio = 0.15

2.5 Sub-basin parameters

Figure 15 shows a map of the defined sub-basins in the Romuku catchment, total 8. For each of these sub-basins, the developed HEC-HMS model requires a set of parameters for the different model components, described previously in Table 1. Table 9 shows the main topographic chacteristics of each sub-basin (area, minimum, average and maximum elevation, and average slope.

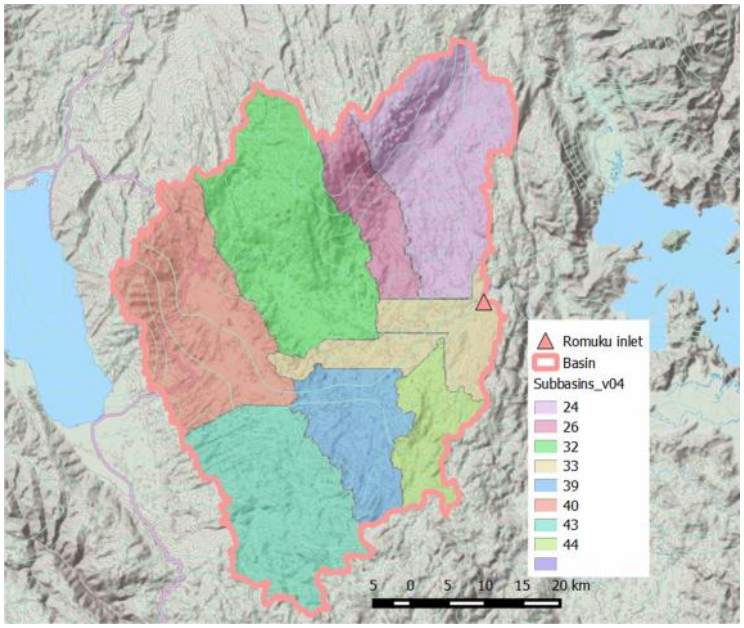

Figure 15. Map of defined sub-basins in the Romuku catchment.

Table 9. Altitude and slope values for the catchments of the Romuku basin.

HYDROID	AREA (km2)	DEM_MIN (m a.s.l.)	DEM_MAX (m a.s.l.)	SLOPE_AVG (%)
24	441	274	2553	17.3
26	152	280	2554	19.6
32	515	274	2344	14.9
33	214	270	1037	8.8
39	214	290	1117	11.8
40	437	407	1284	13.2
43	403	411	1784	17.0
44	140	283	1034	14.2

To use the CN lag method for the within-sub-basin routing of runoff, the HEC-HMS model requires the SCS curve number (CN) to be defined. These were looked up for the combination of Soil Hydrologic Groups and Land Use classes resulting in the area. Representative CN values were assigned to Land Use Classes according the standard look-up table developed by Soil Conservation Service-USDA [*SCS*, 1993], the Hydrological Soil Groups from the soil taxa in the area and expert knowledge criteria (Table 10).

Table 10. CN values for GlobeCover Land Use Cover classes and the Hydrological Soil Groups defined in the study region.

LUC groups	**A**[1)]	**C**[2)]	**D**[3)]
Irrigated croplands	62	81	84
Rainfed croplands	45	77	83
Mosaic cropland / vegetation	67	83	87
Mosaic vegetation / cropland	67	83	87
Closed to open (>15%) forest (>5m)	36	73	79
Closed to open (>15%) shrubland (<5m)	39	74	80
Water bodies	92	92	92

1) HSG A: Ferralsols, Nitisols.

2) HSG C: Kastanozems, Cambisols.

3) HSG D: Acrisols.

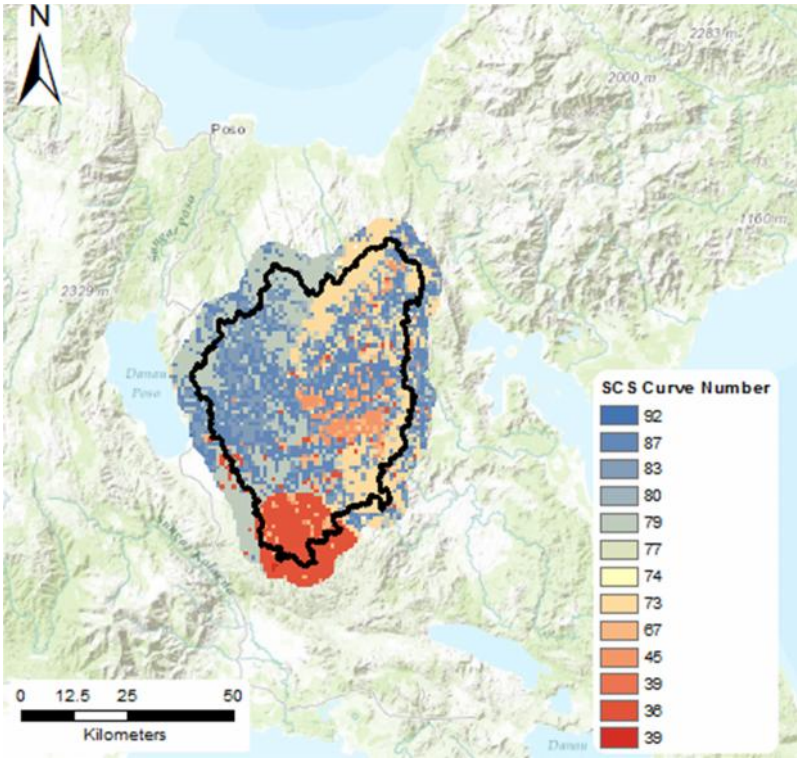

Figure 16. Map of Curve Numbers values in the study basin.

For streamflow routing in the defined reaches (3 in total, as shown in Figure 4), the Muskingum routing method was used, that uses a simple conservation of mass approach to propagate flow through the stream segments. Table 11 shows the parameters that were used for the different reaches. K was calculated using the equation

$K = 1000*L_{ch} / c_k$

where K is the storage time constant of the Muskingum method, L_{ch} is the channel length (km) and c_k is the celerity corresponding to the flow for a specified depth. Celerity can be calculated from an estimate of hydraulic radius and slope. These were interpreted from Google Earth imagery (see also section 3.1).

Table 11. Muskingum routing parameters for the model stream reaches (ordered from upstream to downstream)

Reach code	K (hr)	X
R170	32	0.2
R110	28	0.2
R80	23	0.2

Baseflow parameters are difficult to assess without observed data. The linear reservoir method was used for this study, as it is the only method that conserves mass in HEC-HMS – critical for long-term simulations. No reliable streamflow data are currently available for the area (see following section) but the little data on streamflow does give an indication of the ratio between minimum monthly flow and average flow. Based on this ratio (40%), a discharge per area value can be calculated for the catchment. For this first-order assessment, this discharge per area value was set at 0.024 $m^3/s/km^2$. The groundwater coefficient was calculated assuming active aquifer storage of 500mm and set at 6000 hours.

Maximum storage and infiltration rates were based on soil type, and the values given previously in Table 8.

2.6 Streamflow data

Commonly, model streamflow outputs are checked and calibrated with measured flow data. For this basin, few data were available and for one site. Coordinates of this station were only approximate (1° 58' S, 121° 5' E). They seem to indicate that the measurements have been done somewhere downstream in the basin (Figure 17), but it is not clear whether they were done on the main stem of the river, or a side-branch.

If the station were located on the main stem, total drainage area of this point would be around 1800 km2. With a mean annual rainfall of 2700 mm and a runoff coefficient of 0.5 (which is reasonable in this type of areas, see also section 3.1), this would lead to a an average flow of around 77 m^3/s. Based on the three year monthly data, represented in Figure 18, average flow measured at this station is substantially lower: 28 m3/s.

The reason for this difference may be explained either by wrong measurements (rating curves, etc), or possibly by uncertainty in location: coordinates were approximate, so possibly the measurement location is not on the main stem of the river, but on a side branch (with a smaller draining area).

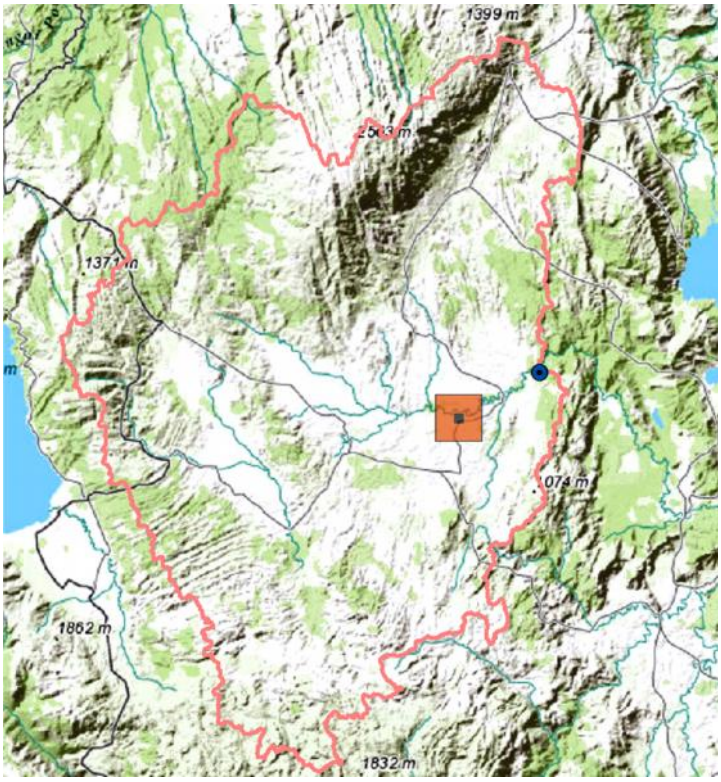

Figure 17. Approximate location of Betapae streamflow measurement point (orange rectangle) of Romuku basin (blue dot)

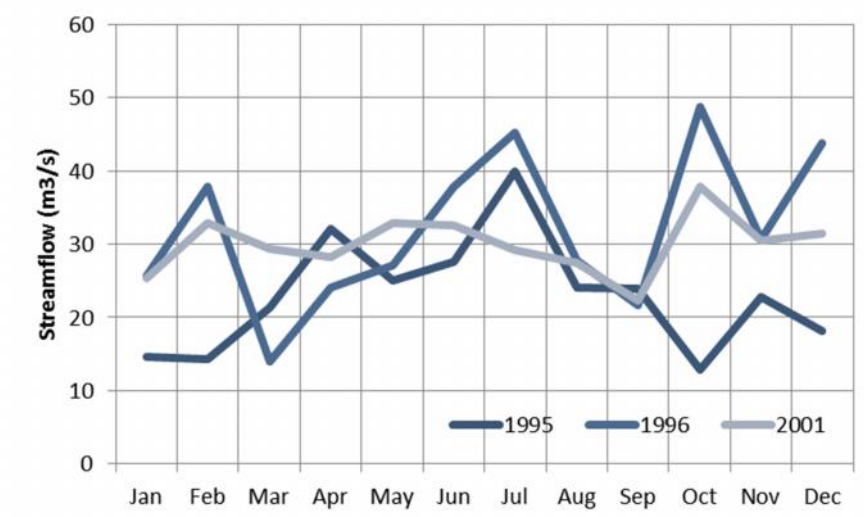

Figure 18. Monthly streamflow of Betapae station within Romuku basin

Given the uncertainty in the location of this measurement point, these data were not used in this pre-feasibility study. Instead, two other indirect methods were used to contrast model output:

- Average streamflow from water balance calculation
- Peak discharges from bankfull discharge estimation

See the result section 3.1 for the details.

2.7 Bounding uncertainties

A pre-feasibility study requires a good understanding of the confidence bounds and the uncertainty that can be expected for the point of interest. At this stage, the main sources of uncertainty are related to:

1. Rainfall patterns and amounts
2. Evapotranspiration
3. Runoff mechanisms , related to rainfall intensities, land use and soil

These uncertainties are typically reduced in hydrological modelling with model calibration using streamflow data. For this study, no reliable streamflow data are available. Therefore, the confidence bounds will be estimated through the model, by generating different scenarios that are within the uncertainty range.

2.7.1 Uncertainty from rainfall

First, uncertainty related to rainfall amounts and patterns is related to the input data from the weather stations, and the TRMM dataset. The selected weather station used as a reference for the area (Mayoa) was considered sufficiently fit for the analysis. Still, a certain amount of error can be expected in the rainfall input dataset due to errors in observations and in the TRMM dataset.

Thus, to assess the confidence bounds related to rainfall observation error, a dry and a wet-period subset was taken from the entire simulation period and flow statistics are calculated for these periods besides the entire period. This leads to 3 scenarios:

- S_full: entire simulation period (1986 – 2013)

- S_dry: dry period, year 1997 – 2004
- S_wet: wet period, year 2005 – 2013

2.7.2 Uncertainty from evapotranspiration

Crop evapotranspiration rates are dependent of a variety of climate factors (temperature, relative humidity, wind). During a rainfall event, the saturation deficit decreases towards zero and crop evapotranspiration is limited. For this reason, hydrological modelling assessments in temperate zones commonly neglect crop evapotranspiration on rainy days.

The tropical climate system however is extremely dynamic and intensive on a sub-daily timescale compared to temperate climate zones. Especially for low intensity rainfall events, evapotranspiration can be significant compared to the rainfall amount. Thus, evapotranspiration can only be neglected during rainfall events exceeding a certain threshold.

To understand how this impacts our flow analysis, two simulations were carried out to assess the uncertainty from evapotranspiration calculations:

- S_evap: neglecting evapotranspiration only when rainfall exceeds 5 mm/day.
- S_evaprain: evapotranspiration occurs independent of rainfall.

2.7.3 Uncertainty from runoff mechanisms

Soil, land use and sub-daily rainfall intensities determine the rainfall-runoff partitioning and thus the attenuation of flow and the shape of the flow duration curve. For this pre-feasibility the best available datasets were used for soil and land use. However, they are global datasets which means that a reasonable amount of uncertainty can be expected, from:

- Spatial patterns
- Classification of soils and land use
- Soil parameters

But even more determining for runoff generation and soil water infiltration, leading to higher uncertainties is rainfall intensity (actual rainfall falling in certain amount of time in mm/hour or mm/min). Data on rainfall intensities are not available, only daily total rainfall amounts. Therefore, it is necessary to make a reasonable assumption on the duration of the rainfall events. Rainfall event duration dynamics are governed by the climate system and can therefore be considered comparable among different sites with the same climate system.

For this study, a reference study was used carried for Central Kalimantan, Indonesia, on the same latitude as the study area, and receiving similar rainfall amounts [*Vernimmen et al.*, 2007]. From this study, the following scenarios were constructed:

- S_short – short events of 1 hour
- S_med – medium events of 2 hours
- S_long – long events of 5 hours

3.1 Streamflow first-order estimates

As a first step in the analysis, this section shows a first-order estimate of streamflow characteristics at the Romuku inlet site, using two methods:

- Simple water balance principles to derive average flow
- Riverbed dimensions of floodplain to derive bankfull discharge

This first-order analysis complements the subsequent modelling outcomes. It gives an a-priori approximation of flow conditions and should add robustness to the analysis.

Average flow from water balance

For long-term assessments, the annual water balance of a basin can be summarized as:

$$P = ETa + Q + A + \Delta S$$

In which P is mean annual precipitation (mm), ETa mean annual actual evapotranspiration (mm), Q mean annual flow (mm), A is possible contribution to or loss from aquifers outside of the hydrographic watershed and ΔS the difference of water stored in the basin in aquifers (storage in soil and other water bodies can be neglected on long-term). The term ΔS becomes relevant when significant amounts of non-renewable water are abstracted from aquifers, which is very likely not the case in this basin. A was neglected for this first-order assessment.

For the Romuku basin, this equation yields:

- Basin size: 2520 km2
- Annual mean basin P: between 2600 – 3200 mm
- Potential ET: between 1200 – 1400 mm, ETa between: 1000 -1400 mm
- Mean flow Q: between 1200 – 2200 mm, or **96 – 176** m3/s

Bankfull discharge

The bank-full discharge at a river cross section is the flow which just fills the channel to the tops of the banks. It is very much related with the cross-sectional shape and size of the channel. Generally, bank full discharge has a return period between 1 and 2 years. To obtain a first-order estimate of bank-full discharge, rough estimates of the cross-section of the river-bed in the floodplain can be used. [*Williams*, 1978] provides general relationships between cross-section and bank-full discharge, based on a 233-station dataset. The equation is as follows:

$$Q_b = 4.0 A_b^{1.21} S^{0.28}$$

In which Qb is bank-full discharge in m3/s, Ab is flow area in m2, and S is slope (dimensionless). For the Romuku basin this yields:

- Width of channel downstream (from Google Earth imagery): 45 m
- Approximate height: between 2 – 4 m, so flow area between 90 and 180 m2
- Bank-full discharge Qb between 134 and 310 m3/s

3.2 Streamflow confidence bounds

This section summarizes the simulations done to bound the uncertainties in the flow duration curve assessment. The Section 3.3 afterwards, wraps this up and shows the final FDC with the confidence bounds.

3.2.1 Uncertainty in rainfall observations

Uncertainty in rainfall data was studied through the simulation model by selecting a period with relatively low rainfall amounts and with high rainfall amounts (see section 2.7). These simulations were done based on medium intense rainfall events (S_med) and allowing evapotranspiration independent of rainfall (S_evaprain) – see section 2.7.

The resulting flow duration curve is shown in Figure 19, with corresponding summary statistics in Table 12.

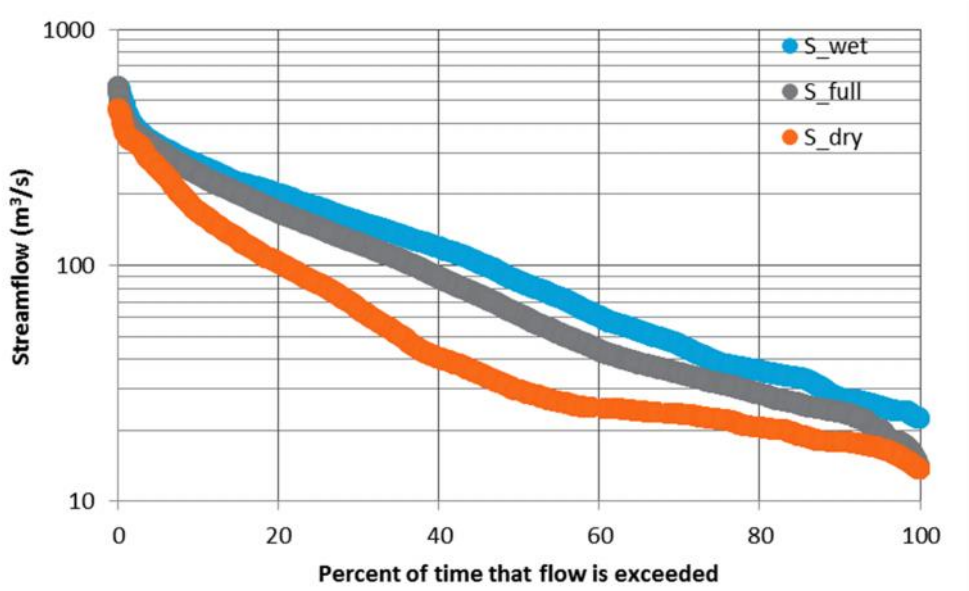

Figure 19. Flow duration curve for uncertainty in rainfall observations: S_full: entire simulation period, S_dry: lowest estimate and S_wet: highest estimate

From the flow duration curve it can be observed that especially the period with low rainfall amounts (S_dry) deviates considerably from the pattern observed for the entire period (S_full). Average flow reduces from around 102 m3/s to 68 m3/s, and the 10%, 50% and 90% percentiles show similar reductions. Follow-up feasibility study should put focus on rainfall data analysis to reduce these uncertainties and obtain more accurate rainfall input data.

Table 12. Summary flow statistics (m^3/s) of rainfall scenarios

	S_full	S_dry	S_wet
Average	102	68	121
90% exceeded	24	18	28
Median	62	30	86
10% exceeded	244	169	268

Monthly flow averages for the three periods of analysis are shown in Figure 20. Based on this modelling assessment, maximum monthly flows (on average between 150 and 200 m^3/s) are expected in April, and minimum flow (between 25 and 50 m^3/s) around September.

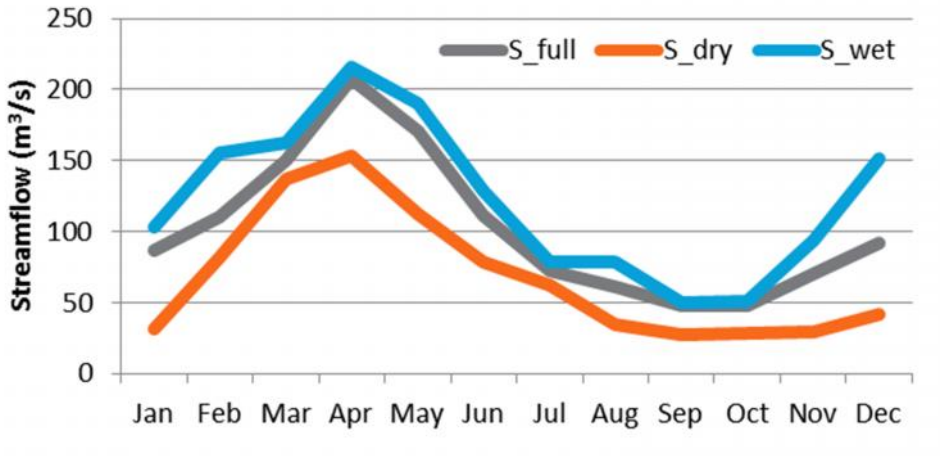

Figure 20. Monthly streamflow for the three rainfall uncertainty scenarios

3.2.2 Uncertainty from evapotranspiration rates

Intensive rainfall events and high evaporative periods can alternate even during one single day in tropical systems. Crop and canopy evapotranspiration is highly dependent on rainfall and other climate variables. Evapotranspiration is therefore another important source of uncertainty for hydrological assessments. This uncertainty was assessed by studying two scenarios (previously discussed):

- Evapotranspiration only when daily rainfall below 5 mm (S_evap)
- Evapotranspiration each day in simulation period, independent of rainfall or not (S_evaprain)

Figure 21 shows the flow duration curve for both simulations. The simulation with evapotranspiration on days < 5mm rainfall shows highest flows (average 148 m^3/s, 50% percentile 108 m^3/s). The S_evaprain simulation has considerable lower flows (average 102 m^3/s, 50% percentile 62 m^3/s)

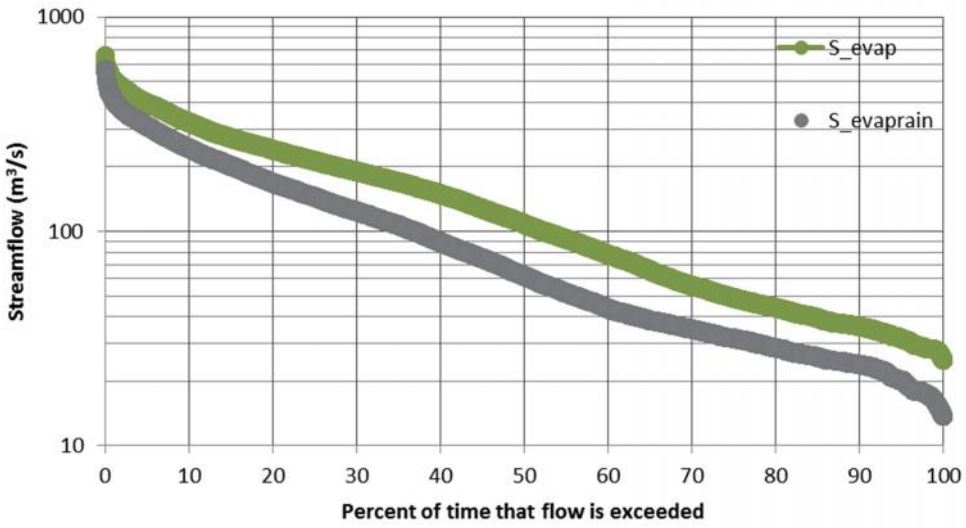

Figure 21. Flow duration curves for uncertainty from evapotranspiration. S_evap: ET on days with less than 5mm rainfall, S_evaprain: simulation with evapotranspiration independent of rainfall

Table 13. Summary flow statistics (m^3/s) of evapotranspiration simulations

	S_evaprain	S_evap
Average	102	148
90% exceeded	24	36
Median	62	108
10% exceeded	244	322

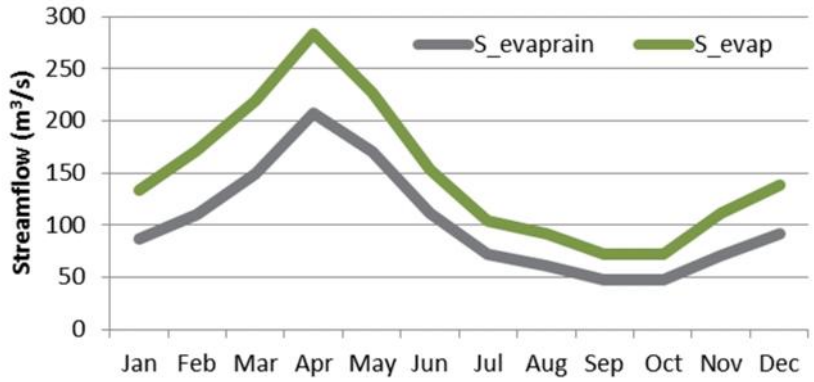

Figure 22. Monthly streamflow for the two evapotranspiration uncertainty simulations

Simulated flow regime is similar among both simulations (Figure 22), but average monthly flows are different, and range between 200 and 280 m^3/s for April, and 50-70 m^3/s for September and October.

3.2.3 Uncertainty from runoff parameters

The rainfall-runoff mechanism depends on rainfall intensities and soil and land cover properties. The related uncertainties were studied assuming different rainfall intensities as discussed previously. The flow duration curve presented in Figure 23 shows mainly differences for the low

flows: for the S_short simulation (rainfall events of 1-hour duration), flows drop below 10 m^3/s and 10% percentile is 14 m^3/s. The S_long simulation (rainfall events on average 5 hours) has a 50% percentile of 72 m^3/s and 10% percentile of 41 m^3/s.

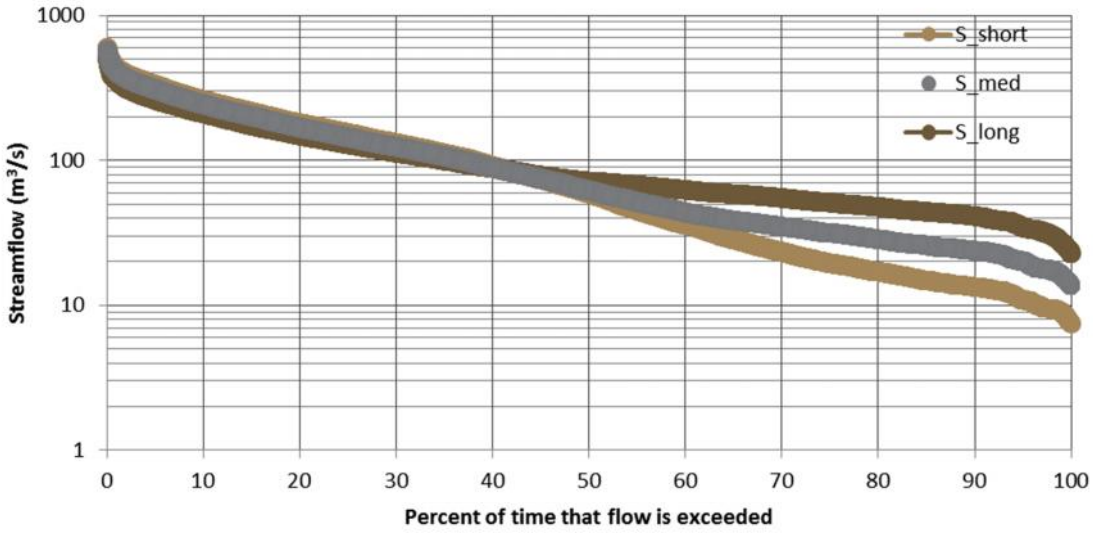

Figure 23. Flow duration curve of simulations assessing influence of uncertainty in runoff mechanism.

Table 14. Summary flow statistics (m^3/s) of evapotranspiration simulations

	S_med	S_short	S_long
Average	102	102	102
90% exceeded	24	14	41
Median	62	59	72
10% exceeded	244	260	212

The monthly streamflow regime is slightly different among the simulations: shorter rainfall events (S_short) give higher peak runoff in months with high rainfall (March-May) , while August-October shows lower streamflow because baseflows are lower. The scenario for less intensive rainfall-runoff events (S_long) shows lower peaks in the high flow season, and higher flows in the low-flow season, as more water infiltrates causing a more regulated flow regime.

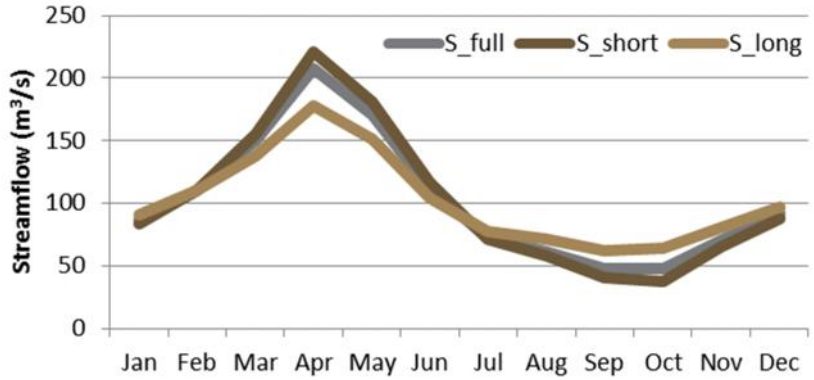

Figure 24. Monthly streamflow for the three runoff uncertainty simulations

3.3 Streamflow summary statistics

From the different simulations, the most likely combination of simulations was chosen: for each of the uncertainty sources the simulation in the middle: S_med, S_evaprain and S_full. Based on this combination, the uncertainty bounds were estimated and plotted (black line in Figure 25).

The confidence bounds were based on the range of outcomes observed in the complete set of simulations. They were estimated for the 10% and the 90% exceedance values, and were assumed to be linear between these extremes. These confidence bounds are indicated in Figure 25 using the greyed area. Table 15 shows the corresponding table for the most likely estimate and the uncertainty bounds from the multiple simulations.

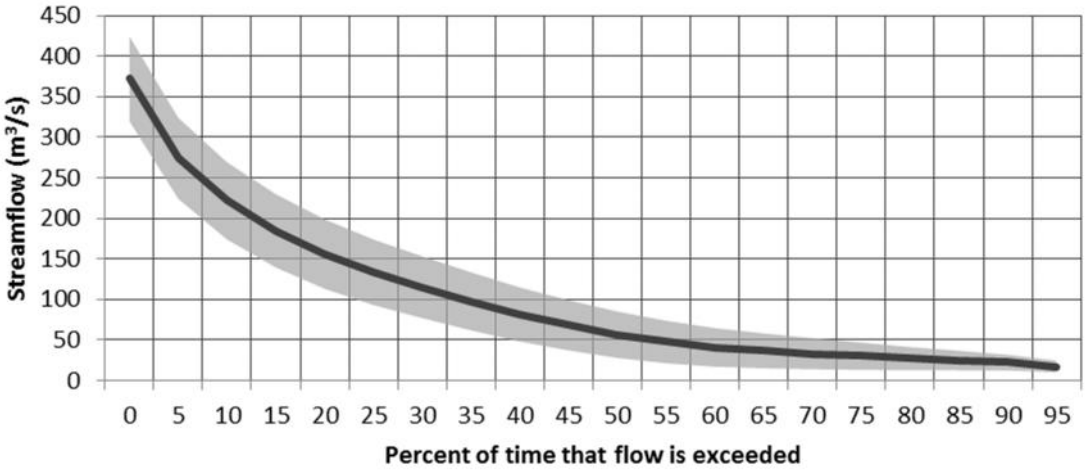

Figure 25. Flow duration curve with confidence bounds based on the uncertainties

Comparing these summary outcomes with the first-order estimates in section 3.1 we can observe the following:

- Flows in the 0-5% bin are similar to the bankfull discharge estimate (higher range): around 350 m3/s on average. This gives confidence to the outcomes of the modelling approach for high flows.
- Average annual flow for the most likely simulation is 104 m3/s. This is on the lower range of first-order estimate carried out using the water balance. Improvements in data and modelling in the feasibility phase can make clear whether this estimate on the lower range was too pessimistic or not.

Overall we can conclude that the above flow duration curve is consistent with the first-order estimates obtained independently without using the hydrological model, in section 3.1.

Table 15. Flow duration table based on the range of simulations in this analysis (m^3/s)

% time flow is exceeded	most likely	lower bound	upper bound
0 - 5	372	320	424
5 - 10	274	224	324
10 - 15	222	174	269
15 - 20	185	140	230
20 - 25	156	113	199
25 - 30	134	93	174
30 - 35	115	77	153
35 - 40	98	62	133
40 - 45	82	48	115
45 - 50	68	37	99
50 - 55	57	28	85
55 - 60	48	21	74
60 - 65	41	17	65
65 - 70	37	15	58
70 - 75	33	14	52
75 - 80	30	13	47
80 - 85	27	13	41
85 - 90	25	13	37
90 - 95	22	13	32
95 - 100	17	10	25

The monthly flow regime at the Romuku inlet is demonstrated in Figure 26, including the uncertainty bounds. These uncertainty bounds were based on the full range that was observed in the multiple model simulations.

The highest uncertainty is found in the high-flow season, where monthly flows may range between 150 and 280 m^3/s. In the low season, average monthly flow range between 30 and 70 m^3/s. Also this approximation of the monthly flow regime can be further improved based on the recommendations in the following sections.

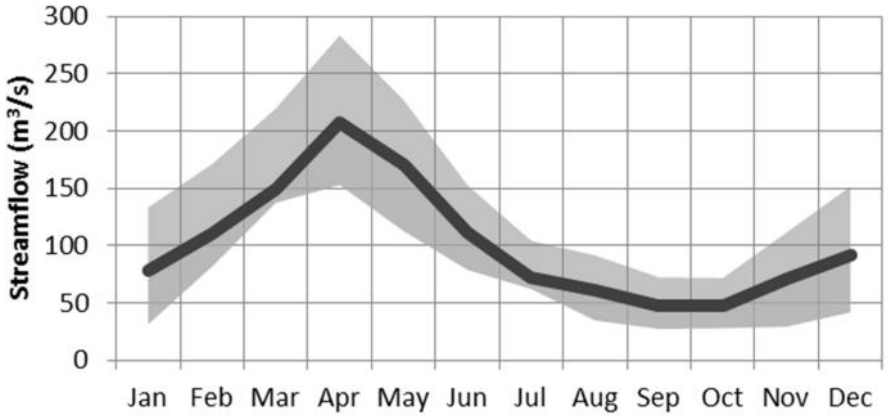

Figure 26. Average monthly flow based on multiple simulations, including confidence bounds

For the most likely simulation, a flood exceedance curve was calculated using the Log Pearson Type III method. Figure 27 shows this curve including confidence bounds that were based only on the most likely simulation (S_med, S_evaprain and S_full). This is important to note, as the bounds shown in this particular figure do not cover the full uncertainty range from rainfall, evapotranspiration and runoff estimation. Similar as for the flow duration curve, the actual uncertainty is around +/- 20% for the simulation time domain.

Based on the simulation data of this pre-feasibility assessment, flood exceedance levels are estimated to be:

- 10 year flood: 500 m^3/s +/- 20%
- 100 year flood: 600 m^3/s +/- 20%
- 1000 year flood: 660 m^3/s +/- 20%

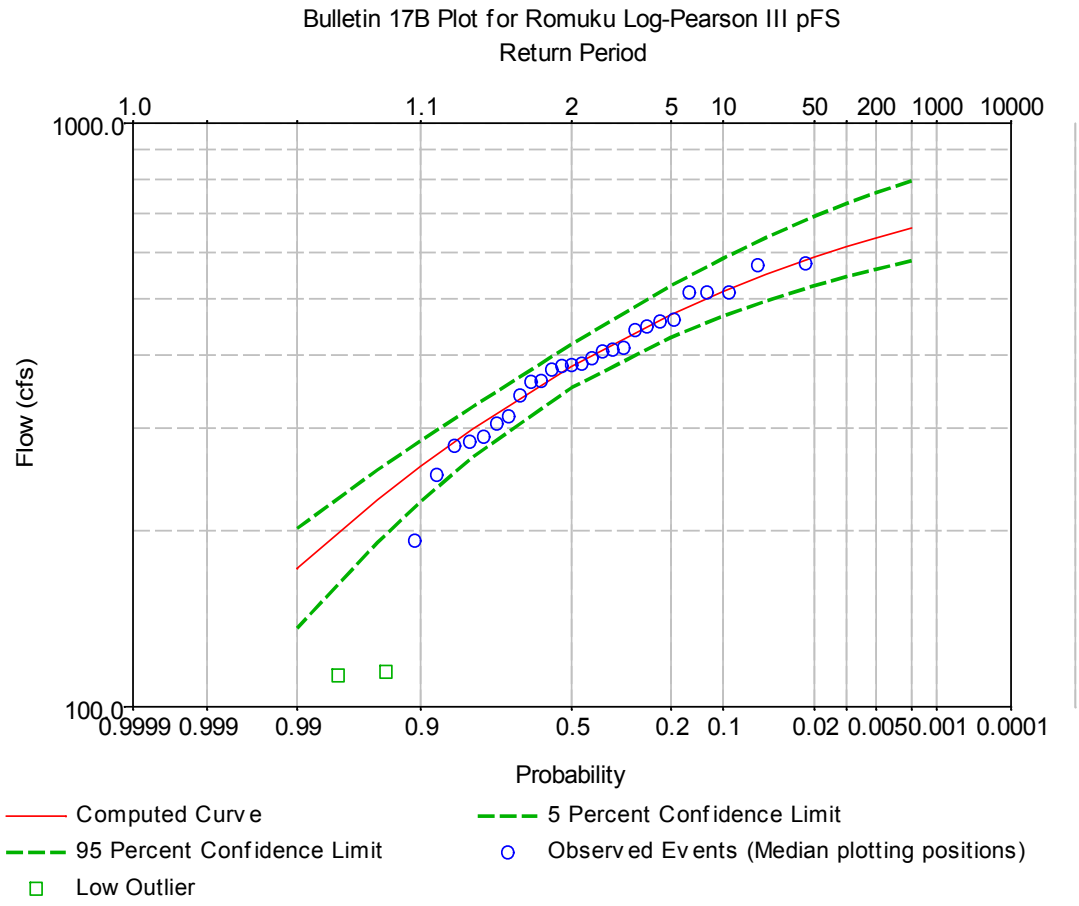

Figure 27. Flood exceedance curve for the most likely simulation

4 Recommendations

This pre-feasibility assessment delivered flow estimates at the Romuku hydropower intake including an estimate of the level of uncertainty. This uncertainty was bounded by studying the main sources of error. The final accuracy level of this assessment is around 10% for the high flows, and 30% for the low flows.

For the following-up feasibility study, it is recommended to reduce this uncertainty and imiprove the accuracy of the analysis. The following improvements are recommended to generate sufficiently detailed outcomes in the following phase, and anticipate a possible design phase:

Data

- Dense vegetation makes digital elevation model SRTM 90m sub-optimal. Some errors were detected in the resulting watershed boundary delimitations. Also flat floodplain areas were not optimally delimited. Improvements are recommended using SRTM 30m in combination with local data on drainage network.
- Land use dataset should be enhanced with supervised classification based on remote sensing data and ground-truth points and optical hi-res imagery (Google Earth, etc). This can greatly increase classification accuracy and thus rainfall-runoff parameterizations.
- Data from Indonesian weather institute or similar on rainfall intensities (even if only available for another but similar area) can enhance accuracy of rainfall-runoff simulation and thus of shape of FDC.
- For this pre-feasibility analysis, monthly TRMM data were used. Daily TRMM should be used in the follow-up phase to further increase accuracy, detect spurious values, and improve the quality of the input rainfall dataset.

Model

- Depending on data improvements, a more advanced model is recommended that allows a more accurate representation of spatial distributions of forcing inputs (rainfall, evapotranspiration) and model parameters (runoff, baseflow, etc). Potential candidates are for example the Soil and Water Assessment Tool (SWAT, http://swat.tamu.edu/), Spatial Process in Hydrology (SPHY www.sphy.nl/), among others
- Given the importance of evapotranspiration in the water balance, more precise modelling of evapotranspiration is recommended using more advanced models (Penmann-Monteith, etc) and validation with estimates from areas with sufficient similarity in biophysical properties.
- Investments in new hydropower infrastructure should be made climate proof, and made robust to possible climate change impacts. Hydrological modelling can reveal how the economic feasibility depends on future changes in climate variability.

Field validation

- The feasibility study requires more precise hydraulic parameters to characterize routing especially during flood and low-flow season. Few-day field survey measuring cross-sectional areas at several points can suffice.
- Flow measurements, even if for short period, could reduce uncertainties in FDC estimation, and can be used to study baseflow recession parameters.

5 References

Alexandersson, H. (1986), A homogeneity test applied to precipitation data, *J. Climatol.*, *6*(6), 661–675, doi:10.1002/joc.3370060607.

FAO (2001), *Lecture notes on the major soils of the world*, Rome.

FAO (2006), *World reference base for soil resources 2006*, Rome.

González-Rouco, J. F., J. L. Jiménez, V. Quesada, and F. Valero (2001), Quality Control and Homogeneity of Precipitation Data in the Southwest of Europe, *J. Clim.*, *14*(5), 964–978, doi:10.1175/1520-0442(2001)014<0964:QCAHOP>2.0.CO;2.

Hengl, T. et al. (2014), SoilGrids1km--global soil information based on automated mapping., *PLoS One*, *9*(8), e105992, doi:10.1371/journal.pone.0105992.

Khaliq, M. N., and T. B. M. J. Ouarda (2007), On the critical values of the standard normal homogeneity test (SNHT), *Int. J. Climatol.*, *27*(5), 681–687, doi:10.1002/joc.1438.

Peterson, T. C. et al. (1998), Homogeneity adjustments ofin situ atmospheric climate data: a review, *Int. J. Climatol.*, *18*(13), 1493–1517, doi:10.1002/(SICI)1097-0088(19981115)18:13<1493::AID-JOC329>3.0.CO;2-T.

SCS (1993), *National Engineering Handbook - Section 4: Hydrology*, Soil Conservation Service - USDA, Washington D.C.

Vernimmen, R. R. E., L. A. Bruijnzeel, A. Romdoni, and J. Proctor (2007), Rainfall interception in three contrasting lowland rain forest types in Central Kalimantan, Indonesia, *J. Hydrol.*, *340*(3-4), 217–232, doi:10.1016/j.jhydrol.2007.04.009.

Wenzel, W. W., H. Unterfrauner, A. Schulte, D. Ruhiyat, D. Simorangkir, V. Kuráz, A. Brandstetter, and W. E. H. Blum (1998), Hydrology of Acrisols beneath Dipterocarp forest and plantations in East Kalimantan, Indonesia, in *Soil of tropical forest ecosystems: Characteristics, ecology and management*, edited by A. Schulte and D. Ruhiyat, pp. 62–72, Springer, Berlin.

Williams, G. P. (1978), Bank-full discharge of rivers, *Water Resour. Res.*, *14*(6), 1141–1154, doi:10.1029/WR014i006p01141.